Information Sciences Letters
An International Journal

http://dx.doi.org/10.18576/isl/090204

Computational analysis of a nonlinear fractional emerging telecommunication model with higher–order dispersive cubic–quintic

Mostafa M.A. Khater[1,2,*], *Raghda A. M. Attia*[2,3] *and Abdel-Haleem Abdel-Aty*[4,5]

[1]Department of Mathematics, El Obour Institutes, Cairo, Egypt
[2]Department of Mathematics, Faculty of Science, Jiangsu University, 212013, China
[3]Department of Basic Science, Higher technological institute 10^{th} of Ramadan city, 44629, Sharkia, Egypt
[4]Department of Physics, College of Sciences, University of Bisha, P.O. Box 344, Bisha 61922, Saudi Arabia
[5]Physics Department, Faculty of Science, Al-Azhar University, 71524 Assiut, Egypt

Received: 13 Jan 2020, Revised: 15 April 2020, Accepted: 19 April 2020
Published online: 1 May 2020

Abstract: In this paper, the modified simplest equation method as one of the computational schemes is applied to a nonlinear fractional emerging telecommunication model with higher-orderer dispersive cubic - quintic for constructing the exact traveling and solitary wave solutions. This model is also known with higher - order dispersive cubic - quintic nonlinear complex fractional Schrödinger ($NLCFS$) equation. Moreover, it is used to explain the physical nature of the waves spread, especially in the dispersive medium. The disadvantages of the B - spline schemes are investigated based on the obtained analytical solutions. Some obtained computational solutions are sketched to more illustration of the wave dynamics in the dispersive medium.

Keywords: Emerging telecommunication model; NLCFS model; Extended simplest equation method; B-spline schemes; Exact traveling and solitary waves solutions.

1 Introduction

Partial differential equations (PDEs) have been playing an essential role in the emerging technologies where many nonlinear evolution equations have been derived to describe the dynamical behavior of several phenomena in several fields, for example, nonlinear optics, fluid dynamics, Bose–Einstein condensates, quantum mechanics and several other areas [1,2,3,4,5,6,7]. However, the inadequate of the PDEs with an–integer order have been clarified because of the nonlocal property where this kind of equation does not explain that kind of features [8,9,10]. Therefore, several natural phenomena have been formulated with nonlinear PDEs with fractional order [11]. Thus, PDEs have been playing an important role in the emerging technologies where many nonlinear evolution equations have been derived to describe the dynamical behaviour of several phenomenon in several fields, for example, nonlinear optics, fluid dynamics, Bose–Einstein condensates, quantum mechanics and several other areas [12,13,14,15]. However, the inadequate of the PDEs with an–integer order have been clarified because of the nonlocal property where this kind of equation do not explain that kind of properties [16,17, 18]. Therefore, several nature phenomena have been formulated with nonlinear PDEs with fractional order [19, 20,21]. Thus, many fractional operators have been derived such as conformable fractional derivative, fractional Riemann–Liouville derivatives, Caputo, Caputo–Fabrizio definition, and so on [22,23,24,25,26].

These definitions have been being employed to convert the fractional nonlinear partial differential equations to a nonlinear integer–order ordinary differential equation. Then the computational and numerical schemes can be applied to get various types of solutions for these models and the examples of these schemes [27,28,29,30,31,32,33,34,35,36,37,38].

This paper studies the analytical and numerical solutions of the $NLCFS$ with higher–order dispersive

* Corresponding author e-mail: mostafa.khater2024@yahoo.com

cubic–quintic arising in the emerging telecommunication [39]. This fractional model describes the wave function or state function of a quantum–mechanical system [40]. Moreover, it is also used in the optical fiber where it occurs in the Manakov system. The NLCFS equation is given by [41,42]

$$\imath\, D_x^{\alpha}\mathcal{U} - \frac{s_1}{2}\,\mathcal{U}_{tt} + r_1\,\mathcal{U}\,|\mathcal{U}|^2 - \imath\,\frac{s_2}{6}\,D_{ttt}^{3\,\alpha}\mathcal{U} - \frac{s_3}{24}\,D_{tttt}^{4\,\alpha}\mathcal{U} + r_2\,\mathcal{U}\,|\mathcal{U}|^4 = 0, \tag{1}$$

where $(0 < \alpha < 1)$, $\mathcal{U}$ describes the propagation of the wave through a nonlinear medium. Additionally, the s_1, s_2 and s_3 are dispersions of order 2^{nd} , 3^{nd} and 4^{nd} respectively, while the r_1 and r_2 are the coefficients of two nonlinearities of the medium, the function q is the gradually varying envelope of the electromagnetic material, the variables t and x are the retarded time and the distance along the direction of propagation respectively. The second and third terms in the above equations are revealed from the velocity dispersion and the Kerr effects. Using the next wave transformation $[\mathcal{U} = \mathcal{U}(x,t) = \mathcal{U}(\mathfrak{Z})\,e^{\imath\,(d_1\,x + d_2\,t + d_3)},\ \mathfrak{Z} = \frac{1}{\alpha}\,(l_1\,x^{\alpha} + l_2\,t^{\alpha})]$ to Eq. (1), yields,

$$\begin{cases} l_2^2\,s_3\,\mathcal{U}^{(4)} + \left(12\,s_1\,l_2^2 - 6\,s_3\,d_2^2\,l_2^2 - 12\,s_2\,d_2\,l_2^2\right)\mathcal{U}'' + \left(s_3\,d_2^4 + 4\,s_2\,d_1^3 - 12\,s_1\,d_2 + 24\,d_1\right)\mathcal{U} - 24\,r_2\,\mathcal{U}^5 - 24\,r_1\,\mathcal{U}^3 = 0, \\ \left(-4\,s_3\,d_2^3\,l_2 - 12\,s_2\,d_2^2\,l_2 + 24\,s_1\,d_2\,l_2 - 24\,k_1\right)\mathcal{U}' + 4\,l_2^3\,\left(s_3\,d_2 + s_2\right)\mathcal{U}''' = 0, \end{cases} \tag{2}$$

where $[d_i,\, l_j,\, (i = 1,2,3),\, (j = 1,2)]$ are arbitrary constants. Differentiating second equation of the system (2) and then substitute the result into the first equation of the same equation, gives

$$k_1\,\mathcal{U}'' + k_2\,\mathcal{U}^5 + k_3\,\mathcal{U}^3 + k_4\,\mathcal{U} = 0, \tag{3}$$

where

$$\begin{aligned} k_1 &= l_2^2\left(12 s_1 - 6 s_3\,d_2^2 - 12\,s_2\,d_2\right) \\ &\quad\times\left(\frac{4\,s_3\,d_2^3\,l_2 + 12\,s_3\,d_2^2\,l_2 - 24\,s_1\,d_2\,l_2 + 24\,k_1}{4\,l_2^3\,\left(s_3\,d_2 + s_2\right)}\right), \\ k_2 &= -24\,r_2,\ k_3 = -24\,r_1, \\ k_4 &= \left(s_3\,d_2^4 + 4\,s_2\,d_2^3 - 12\,s_1\,d_2^2 + 24\,d_1\right) \end{aligned}$$

Applying the homogeneous balance principle to Eq. (3), leads to $(m = \frac{1}{2})$. Thus, we use the next transformation $[\mathcal{U} = \mathcal{Q}^{\frac{1}{2}}]$ to the Eq. (3), yields

$$\frac{-k_1}{4}\,\mathcal{Q}'^2 + \frac{k_1}{2}\,\mathcal{Q}\,\mathcal{Q}'' + k_2\,\mathcal{Q}^4 + k_3\,\mathcal{Q}^3 + k_4\,\mathcal{Q}^2 = 0. \tag{4}$$

Applying the homogeneous balance principle to Eq. (4), obtains $(m = 1)$.

The rest of research paper is organized as follows: Section (2), applies the extended simplest equation method and B - spline schemes to the suggested model to get exact traveling and solitary wave solutions of it [43, 44,45,46,47,48,49]. Section (4), explains the conclusion of all the steps of our paper is detailed.

2 Application

Here in this section, the extended simplest equation method and B - spline schemes are applied to the NLCFS equation t;o explain the restricted electromagnetic wave which stretches in media of nonlinear dispersive. Due to stability among nonlinearity and dispersion effects, the intensity of optical solitons are unchanged, and such categories of solitary waves are more significant because of their suppleness in optical of long distance.

2.1 Computational solutions

Applying the extended simplest equation method to Eq. (4), leads to formulate the general solution of this model in the following formula

$$\mathcal{Q}(\mathfrak{Z}) = \sum_{i=-n}^{n} a_i\,\mathcal{F}^i(\mathfrak{Z}) = \frac{a_{-1}}{\mathcal{F}(\mathfrak{Z})} + a_1\mathcal{F}(\mathfrak{Z}) + a_0, \tag{5}$$

where $[a_{-1},\, a_0,\, a_1]$ are arbitrary constants to be determined later. Additionally, $\mathcal{F}(\mathfrak{Z})$ is the solution function of the following ordinary differential equation

$$\mathcal{F}'(\mathfrak{Z}) = \alpha + \lambda\,\mathcal{F}(\mathfrak{Z}) + \mu\,\mathcal{F}(\mathfrak{Z})^2, \tag{6}$$

where $[\alpha,\, \lambda,\, \mu]$ are arbitrary constant. Substituting Eq. (5) along (6) into Eq. (4) and collecting all terms with the same power of $[\mathcal{F}^i(\mathfrak{Z}),\, i = -5,-4,...,4,5]$, give a system of algebraic equation. Using the Mathematica 12 program for solving this system, yields

Family I:

$[a_{-1} \to \frac{\alpha a_0}{\lambda}, a_1 \to \frac{a_0 \mu}{\lambda}, k_2 \to -\frac{3\lambda^2 k_1}{4a_0^2}, k_3 \to \frac{\lambda^2 k_1}{a_0}, k_4 \to -\frac{1}{4}k_1\left(\lambda^2 - 4\alpha\mu\right)]$

Thus, the explicit wave solutions of Eq. (1) are formulated in the following formulas

For $[\alpha = 0]$ when $(\lambda > 0)$

$$\mathcal{U}_1 = e^{id_2 t + id_1 x + id_3}\sqrt{\frac{a_0}{1 - \mu e^{\lambda(\xi+\vartheta)}}}. \tag{7}$$

When $(\lambda < 0)$

$$\mathcal{U}_2 = e^{id_2 t + id_1 x + id_3}\sqrt{a_0\left(1 - \frac{\mu - \frac{\mu}{\mu e^{\lambda(\xi+\vartheta)}+1}}{\lambda}\right)}. \tag{8}$$

For $[4\,\alpha\,\mu > \lambda^2]$,

$$\mathcal{U}_3 = e^{id_2 t + id_1 x + id_3}\sqrt{\frac{a_0\left(\lambda^2 - 4\alpha\mu\right)}{\lambda\left(-\sqrt{4\alpha\mu - \lambda^2}\sin\left((\xi+\vartheta)\sqrt{4\alpha\mu-\lambda^2}\right) + \lambda\cos\left((\xi+\vartheta)\sqrt{4\alpha\mu-\lambda^2}\right) + \lambda\right)}}, \tag{9}$$

$$\mathcal{U}_4 = e^{id_2 t + id_1 x + id_3}\sqrt{-\frac{a_0\left(\lambda^2 - 4\alpha\mu\right)}{\lambda\left(\sqrt{4\alpha\mu - \lambda^2}\sin\left((\xi+\vartheta)\sqrt{4\alpha\mu-\lambda^2}\right) + \lambda\cos\left((\xi+\vartheta)\sqrt{4\alpha\mu-\lambda^2}\right) - \lambda\right)}}. \tag{10}$$

Family II:

$[a_{-1} \to \frac{\sqrt{\alpha}a_0}{2\sqrt{\mu}}, a_1 \to \frac{a_0\sqrt{\mu}}{2\sqrt{\alpha}}, k_2 \to -\frac{3\alpha k_1 \mu}{a_0^2}, k_3 \to \frac{k_1\left(8\alpha\mu - 2\sqrt{\alpha}\lambda\sqrt{\mu}\right)}{a_0}, k_4 \to \frac{1}{4}\left(12\sqrt{\alpha}k_1\lambda\sqrt{\mu} - 20\alpha k_1\mu - \lambda^2 k_1\right)]$

Thus, the explicit wave solutions of Eq. (1) are formulated in the following formulas

For $[\lambda = 0]$, when $(\alpha\,\mu > 0)$

$$\mathcal{U}_5 = e^{id_2 t + id_1 x + id_3}\sqrt{a_0\left(\csc\left(2\sqrt{\alpha}\sqrt{\mu}(\xi+\vartheta)\right) + 1\right)}. \tag{11}$$

When $(\alpha\,\mu < 0)$

$$\mathcal{U}_6 = e^{id_2 t + id_1 x + id_3}\sqrt{a_0\left(\frac{\sqrt{\alpha}\sqrt{\mu}\,\mathrm{csch}\left(2\left(\xi\sqrt{-\alpha\mu} \mp \frac{\log(\vartheta)}{2}\right)\right)}{\sqrt{-\alpha\mu}} + 1\right)}. \tag{12}$$

For $[4\alpha\mu > \lambda^2]$

$$\mathcal{U}_7 = \frac{1}{2}e^{id_2 t + id_1 x + id_3}\sqrt{-\frac{a_0\left(-2\sqrt{\alpha}\sqrt{\mu} - \sqrt{4\alpha\mu - \lambda^2}\tan\left(\frac{1}{2}(\xi+\vartheta)\sqrt{4\alpha\mu-\lambda^2}\right) + \lambda\right)^2}{\sqrt{\alpha}\sqrt{\mu}\left(\lambda - \sqrt{4\alpha\mu-\lambda^2}\tan\left(\frac{1}{2}(\xi+\vartheta)\sqrt{4\alpha\mu-\lambda^2}\right)\right)}}, \tag{13}$$

$$\mathcal{U}_8 = \frac{1}{2}e^{id_2 t + id_1 x + id_3}\sqrt{-\frac{a_0\left(-2\sqrt{\alpha}\sqrt{\mu} - \sqrt{4\alpha\mu - \lambda^2}\cot\left(\frac{1}{2}(\xi+\vartheta)\sqrt{4\alpha\mu-\lambda^2}\right) + \lambda\right)^2}{\sqrt{\alpha}\sqrt{\mu}\left(\lambda - \sqrt{4\alpha\mu-\lambda^2}\cot\left(\frac{1}{2}(\xi+\vartheta)\sqrt{4\alpha\mu-\lambda^2}\right)\right)}}. \tag{14}$$

Family III:

$[a_{-1} \to \frac{\sqrt{a_0^2(\lambda^2-4\alpha\mu)}+a_0\lambda}{2\mu}, a_1 \to 0, k_2 \to \frac{3k_1\left(\lambda\sqrt{a_0^2(\lambda^2-4\alpha\mu)}-a_0\left(\lambda^2-2\alpha\mu\right)\right)}{8a_0^3},$
$k_3 \to \frac{k_1\left(a_0\left(\lambda^2-4\alpha\mu\right)-\lambda\sqrt{a_0^2(\lambda^2-4\alpha\mu)}\right)}{2a_0^2}, k_4 \to -\frac{1}{4}k_1\left(\lambda^2-4\alpha\mu\right)]$

Thus, the explicit wave solutions of Eq. (1) are formulated in the following formulas.

For $[\lambda = 0]$ when $(\alpha\mu < 0)$

$$\mathcal{U}_9 = e^{id_2t+id_1x+id_3}\sqrt{\frac{\sqrt{-\alpha a_0^2\mu}\coth\left(\xi\sqrt{-\alpha\mu}\mp\frac{\log(\vartheta)}{2}\right)}{\sqrt{-\alpha\mu}}+a_0}, \tag{15}$$

$$\mathcal{U}_{10} = e^{id_2t+id_1x+id_3}\sqrt{\frac{\sqrt{-\alpha a_0^2\mu}\tanh\left(\xi\sqrt{-\alpha\mu}\mp\frac{\log(\vartheta)}{2}\right)}{\sqrt{-\alpha\mu}}+a_0}. \tag{16}$$

For $[\alpha = 0]$ when $(\lambda > 0)$

$$\mathcal{U}_{11} = e^{id_2t+id_1x+id_3}\sqrt{a_0-\frac{\left(\sqrt{a_0^2\lambda^2}+a_0\lambda\right)e^{-\lambda(\xi+\vartheta)}\left(\mu e^{\lambda(\xi+\vartheta)}-1\right)}{2\lambda\mu}}. \tag{17}$$

Family IV:

$\left[a_{-1} \to 0, a_1 \to \frac{a_0\lambda-\sqrt{a_0^2\lambda^2-4\alpha a_0^2\mu}}{2\alpha}, k_2 \to -\frac{3k_1\left(\lambda\sqrt{a_0^2(\lambda^2-4\alpha\mu)}+a_0\left(\lambda^2-2\alpha\mu\right)\right)}{8a_0^3}, k_3 \to \frac{k_1\left(\lambda\sqrt{a_0^2(\lambda^2-4\alpha\mu)}+a_0\left(\lambda^2-4\alpha\mu\right)\right)}{2a_0^2},\right.$
$\left.k_4 \to -\frac{1}{4}k_1\left(\lambda^2-4\alpha\mu\right)\right]$

Thus, the explicit wave solutions of Eq. (1) are formulated in the following formulas

For $[\lambda = 0]$ when $(\alpha\mu < 0)$

$$\mathcal{U}_{12} = e^{id_2t+id_1x+id_3}\sqrt{\frac{\sqrt{-\alpha a_0^2\mu}\tanh\left(\xi\sqrt{-\alpha\mu}\mp\frac{\log(\vartheta)}{2}\right)}{\sqrt{-\alpha\mu}}+a_0}, \tag{18}$$

$$\mathcal{U}_{13} = e^{id_2t+id_1x+id_3}\sqrt{\frac{\sqrt{-\alpha a_0^2\mu}\coth\left(\xi\sqrt{-\alpha\mu}\mp\frac{\log(\vartheta)}{2}\right)}{\sqrt{-\alpha\mu}}+a_0}. \tag{19}$$

2.2 Numerical solutions

Here, we try to find the numerical solutions of the *NLCFS* equation via the B - spline schemes as following

2.2.1 Cubic B–Spline

Employing the cubic spline technique to Eq. (4) with the above conditions, yields elicit its numerical solutions as following

$$\mathfrak{P}(\mathfrak{Z}) = \sum_{\mathfrak{T}=-1}^{\mathfrak{M}+1} \mathfrak{C}_{\mathfrak{T}}\,\mathcal{E}_{\mathfrak{T}}, \tag{20}$$

where $\mathfrak{C}_{\mathfrak{T}}$, $\mathcal{E}_{\mathfrak{T}}$ follow the next conditions, respectively:

$$\mathfrak{L}\,\mathfrak{B}(\mathfrak{Z}) = \mathcal{F}(\mathfrak{Z}_{\mathfrak{T}}, \mathfrak{B}(\mathfrak{Z}_{\mathfrak{T}})) \text{ where } (\mathfrak{T} = 0, 1, ..., n) \tag{21}$$

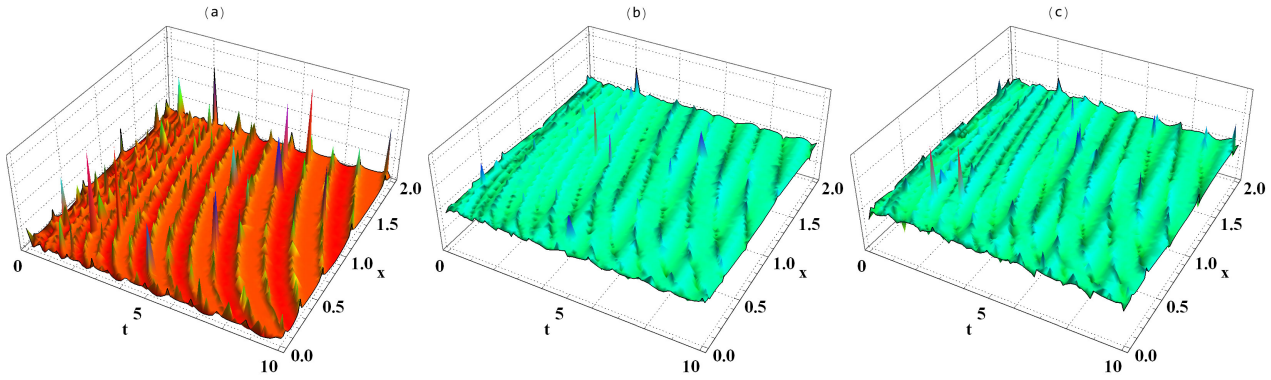

Fig. 1: Numerical simulation of Eq. (4) in three–dimensional sketches.

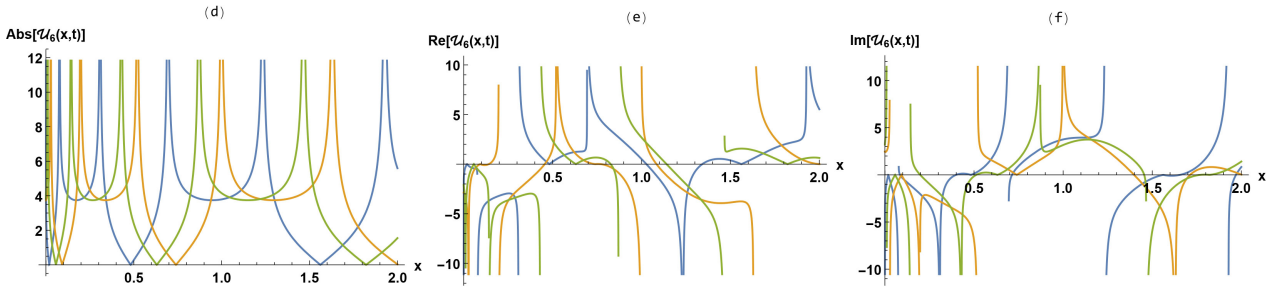

Fig. 2: Numerical simulation of Eq. (4) in two–dimensional sketches.

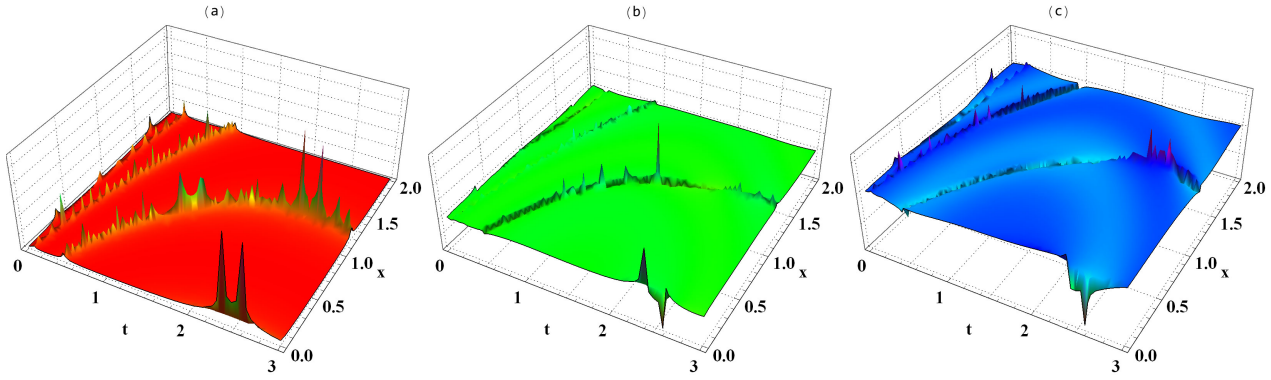

Fig. 3: Numerical simulation of Eq. (4) in three–dimensional sketches.

and

$$\mathcal{E}_{\mathfrak{T}}(\mathfrak{Z}) = \frac{1}{6\,\mathfrak{H}^3}\begin{cases} (\mathfrak{Z}-\mathfrak{Z}_{\mathfrak{T}-2})^3, & \mathfrak{Z}\in[\mathfrak{Z}_{\mathfrak{T}-2},\mathfrak{Z}_{\mathfrak{T}-1}],\\ -3\,(\mathfrak{Z}-\mathfrak{Z}_{\mathfrak{T}-1})^3+3\,\mathfrak{H}\,(\mathfrak{Z}-\mathfrak{Z}_{\mathfrak{T}-1})^2+3\,\mathfrak{H}^2\,(\mathfrak{Z}-\mathfrak{Z}_{\mathfrak{T}-1})+\mathfrak{H}^3, & \mathfrak{Z}\in[\mathfrak{Z}_{\mathfrak{T}-1},\mathfrak{Z}_i],\\ -3\,(\mathfrak{Z}_{\mathfrak{T}+1}-\mathfrak{Z})^3+3\,\mathfrak{H}\,(\mathfrak{Z}_{\mathfrak{T}+1}-\mathfrak{Z})^2+3\,\mathfrak{H}^2\,(\mathfrak{Z}_{\mathfrak{T}+1}-\mathfrak{Z})+\mathfrak{H}^3, & \mathfrak{Z}\in[\mathfrak{Z}_{\mathfrak{T}},\mathfrak{Z}_{\mathfrak{T}+1}],\\ (\mathfrak{Z}_{\mathfrak{T}+2}-\mathfrak{Z})^3, & \mathfrak{Z}\in[\mathfrak{Z}_{\mathfrak{T}+1},\mathfrak{Z}_{\mathfrak{T}+2}],\\ 0, & \text{otherwise.}\end{cases} \tag{22}$$

For $\mathfrak{T}\in[-2,\mathfrak{M}+2]$, we obtain

$$\mathfrak{B}_{\mathfrak{T}}(\mathfrak{Z}) = \mathfrak{C}_{\mathfrak{T}-1}+4\,\mathfrak{C}_{\mathfrak{T}}+\mathfrak{C}_{\mathfrak{T}+1}. \tag{23}$$

Substituting Eq. (23) into Eq. (4), yields $(\mathfrak{M}+3)$ of equations. Resolving this system gives the results in table 1.

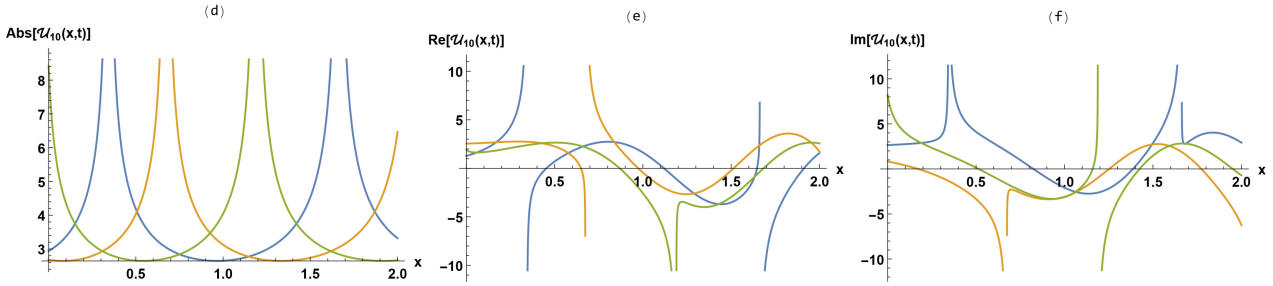

Fig. 4: Numerical simulation of Eq. (4) in two–dimensional sketches.

2.2.2 Quantic B–spline

Employing the cubic spline technique to Eq. (4) with the above conditions gives its numerical solutions in the next formula

$$\mathfrak{B}(\mathfrak{Z}) = \sum_{\mathfrak{M}=-1}^{\mathfrak{M}+1} \mathfrak{C}_{\mathfrak{T}}\, \mathcal{E}_{\mathfrak{T}}, \tag{24}$$

where $\mathfrak{C}_{\mathfrak{T}}$, $\mathcal{E}_{\mathfrak{T}}$ follow the next conditions, respectively:

$$\mathfrak{L}\,\mathfrak{B}(\mathfrak{Z}) = \mathcal{F}(\mathfrak{Z}_{\mathfrak{T}}, \mathfrak{B}(\mathfrak{Z}_{\mathfrak{T}})) \text{ where } (\mathfrak{T} = 0, 1, ..., n) \tag{25}$$

and

$$\mathcal{E}_{\mathfrak{T}}(\mathfrak{Z}) = \frac{1}{\mathfrak{h}^5} \begin{cases} (\mathfrak{Z} - \mathfrak{Z}_{\mathfrak{T}-3})^5, & \mathfrak{Z} \in [\mathfrak{Z}_{\mathfrak{T}-3}, \mathfrak{Z}_{\mathfrak{T}-2}], \\ (\mathfrak{Z} - \mathfrak{Z}_{\mathfrak{T}-3})^5 - 6(\mathfrak{Z} - \mathfrak{Z}_{\mathfrak{T}-2})^5, & \mathfrak{Z} \in [\mathfrak{Z}_{\mathfrak{T}-2}, \mathfrak{Z}_{\mathfrak{T}-1}], \\ (\mathfrak{Z} - \mathfrak{Z}_{\mathfrak{T}-3})^5 - 6(\mathfrak{Z} - \mathfrak{Z}_{\mathfrak{T}-2})^5 + 15(\mathfrak{Z} - \mathfrak{Z}_{\mathfrak{T}-1})^5, & \mathfrak{Z} \in [\mathfrak{Z}_{\mathfrak{T}-1}, \mathfrak{Z}_{\mathfrak{T}}], \\ (\mathfrak{Z}_{\mathfrak{T}+3} - \mathfrak{Z})^5 - 6(\mathfrak{Z}_{\mathfrak{T}+2} - \mathfrak{Z})^5 + 15(\mathfrak{Z}_{\mathfrak{T}+1} - \mathfrak{Z})^5, & \mathfrak{Z} \in [\mathfrak{Z}_{\mathfrak{T}}, \mathfrak{Z}_{\mathfrak{T}+1}], \\ (\mathfrak{Z}_{\mathfrak{T}+3} - \mathfrak{Z})^5 - 6(\mathfrak{Z}_{\mathfrak{T}+2} - \mathfrak{Z})^5, & \mathfrak{Z} \in [\mathfrak{Z}_{\mathfrak{T}+1}, \mathfrak{Z}_{\mathfrak{T}+2}], \\ (\mathfrak{Z}_{\mathfrak{T}+3} - \mathfrak{Z})^5, & x \in [\mathfrak{Z}_{\mathfrak{T}+2}, \mathfrak{Z}_{\mathfrak{T}+3}], \\ 0, & \text{otherwise.} \end{cases} \tag{26}$$

For $\mathfrak{T} \in [-2, \mathfrak{M}+2]$, we get

$$\mathfrak{B}_{\mathfrak{T}}(\mathfrak{Z}) = \mathfrak{C}_{\mathfrak{T}-2} + 26\,\mathfrak{C}_{\mathfrak{T}-1} + 66\,\mathfrak{C}_{\mathfrak{T}} + 26\,\mathfrak{C}_{\mathfrak{T}+1} + \mathfrak{C}_{\mathfrak{T}+2}. \tag{27}$$

Substituting Eq. (27) into Eq. (4) gives $(\mathfrak{M}+5)$ of equations. Resolving this system, leads to the results in table 2.

2.2.3 Septic B–Spline

Employing the septic spline technique to Eq. (4) with the above conditions gives its numerical solutions in the next form

$$\mathfrak{B}(\mathfrak{Z}) = \sum_{\mathfrak{T}=-1}^{\mathfrak{M}+1} \mathfrak{C}_{\mathfrak{M}}\, \mathcal{E}_{\mathfrak{M}}, \tag{28}$$

where $c_{\mathfrak{M}}$, $\mathcal{E}_{\mathfrak{M}}$ follow the next conditions, respectively:

$$\mathfrak{L}\,\mathfrak{B}(\mathfrak{Z}) = \mathcal{F}(\mathfrak{Z}_{\mathfrak{M}}, \mathfrak{B}(\mathfrak{Z}_{\mathfrak{M}})) \text{ where } (\mathfrak{M} = 0, 1, ..., n) \tag{29}$$

Table 1: Value of exact solutions, and numerical obtained solutions by cubic spline scheme of (4) under the following conditions $[a_0 = 2,\ \alpha = -1,\ \lambda = 0,\ k_1 = 3,\ k_2 = -\frac{9}{4},\ k_3 = 12,\ k_4 = -12,\ \mu = 4,\ \vartheta = 1]$ for Eq. (16)

Value of $\mathfrak{Z}$	Exact value	Numerical Value	Absolute error
0	2	2	0
0.1	2.39475	0.994884	1.39987
0.2	2.7599	0.335965	2.42393
0.3	3.0741	0.0302715	3.04383
0.4	3.32807	-0.00460121	3.33267
0.5	3.52319	-0.000604126	3.52379
0.6	3.66731	-0.0137043	3.68101
0.7	3.7707	0.0684398	3.70226
0.8	3.84334	0.707378	3.13596
0.9	3.89361	2.02339	1.87023
1	3.92806	3.92806	0

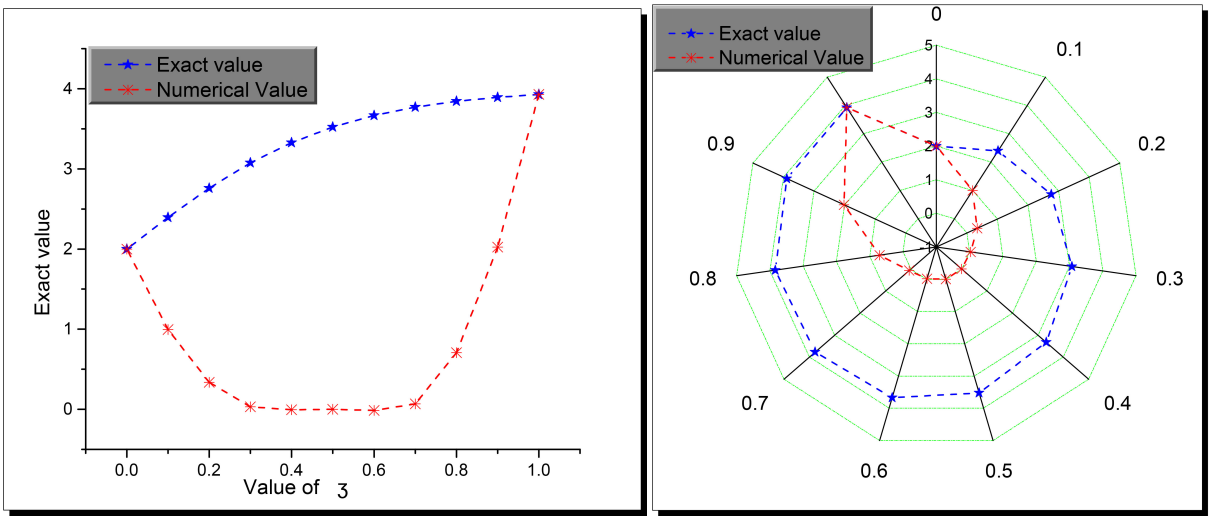

Fig. 5: Exact and numerical values by using cubic B–spline scheme for the three analytical schemes

and

$$\mathcal{E}_{\mathfrak{T}}(\mathfrak{Z}) = \frac{1}{\mathfrak{H}^5}\begin{cases} (\mathfrak{Z}-\mathfrak{Z}_{\mathfrak{T}-4})^7, & \mathfrak{Z}\in[\mathfrak{Z}_{\mathfrak{T}-4},\mathfrak{Z}_{\mathfrak{T}-3}],\\ (\mathfrak{Z}-\mathfrak{Z}_{\mathfrak{T}-4})^7-8(\mathfrak{Z}-\mathfrak{Z}_{\mathfrak{T}-3})^7, & \mathfrak{Z}\in[\mathfrak{Z}_{\mathfrak{T}-3},\mathfrak{Z}_{\mathfrak{T}-2}],\\ (\mathfrak{Z}-\mathfrak{Z}_{\mathfrak{T}-4})^7-8(\mathfrak{Z}-\mathfrak{Z}_{\mathfrak{T}-3})^7+28(\mathfrak{Z}-\mathfrak{Z}_{\mathfrak{T}-2})^7, & \mathfrak{Z}\in[\mathfrak{Z}_{\mathfrak{T}-2},\mathfrak{Z}_{\mathfrak{T}-1}],\\ (\mathfrak{Z}-\mathfrak{Z}_{\mathfrak{T}-4})^7-8(\mathfrak{Z}-\mathfrak{Z}_{\mathfrak{T}-3})^7+28(\mathfrak{Z}-\mathfrak{Z}_{\mathfrak{T}-2})^7+56(\mathfrak{Z}-\mathfrak{Z}_{\mathfrak{T}-1})^7, & \mathfrak{Z}\in[\mathfrak{Z}_{\mathfrak{T}-1},\mathfrak{Z}_{\mathfrak{T}}],\\ (\mathfrak{Z}_{\mathfrak{T}+4}-\mathfrak{Z})^7-8(\mathfrak{Z}_{\mathfrak{T}+3}-\mathfrak{Z})^7+28(\mathfrak{Z}_{\mathfrak{T}+2}-\mathfrak{Z})^7+56(\mathfrak{Z}_{\mathfrak{T}+1}-\mathfrak{Z})^7, & \mathfrak{Z}\in[\mathfrak{Z}_{\mathfrak{T}},\mathfrak{Z}_{\mathfrak{T}+1}],\\ (\mathfrak{Z}_{\mathfrak{T}+4}-\mathfrak{Z})^7-8(\mathfrak{Z}_{\mathfrak{T}+3}-\mathfrak{Z})^7+28(\mathfrak{Z}_{\mathfrak{T}+2}-\mathfrak{Z})^7, & \mathfrak{Z}\in[\mathfrak{Z}_{\mathfrak{T}+1},\mathfrak{Z}_{\mathfrak{T}+2}],\\ (\mathfrak{Z}_{\mathfrak{T}+4}-\mathfrak{Z})^7-8(\mathfrak{Z}_{\mathfrak{T}+3}-\mathfrak{Z})^7, & \mathfrak{Z}\in[\mathfrak{Z}_{\mathfrak{T}+2},\mathfrak{Z}_{\mathfrak{T}+3}],\\ (\mathfrak{Z}_{\mathfrak{T}+4}-\mathfrak{Z})^7, & \mathfrak{Z}\in[\mathfrak{Z}_{\mathfrak{T}+3},\mathfrak{Z}_{\mathfrak{T}+4}],\\ 0, & \text{otherwise.}\end{cases} \tag{30}$$

For $\mathfrak{T}\in[-3,\mathfrak{M}+3]$, we get

$$\begin{aligned}\mathfrak{B}_{\mathfrak{T}}(\mathfrak{Z}) = {} & \mathfrak{C}_{\mathfrak{T}-3}+120\,\mathfrak{C}_{\mathfrak{T}-2}+1191\,\mathfrak{C}_{\mathfrak{T}-1}+2416\,\mathfrak{C}_{\mathfrak{T}}\\ & +1191\,\mathfrak{C}_{\mathfrak{T}+1}+120\,\mathfrak{C}_{\mathfrak{T}+2}+\mathfrak{C}_{\mathfrak{T}+3}.\end{aligned} \tag{31}$$

Substituting Eq. (31) into Eq. (4) gives $(\mathfrak{M}+7)$ of equations. Resolving this system leads to the results in table (3).

Table 2: Value of exact solutions, and numerical obtained solutions by quantic spline scheme of (4) under the following conditions $[a_0 = 2,\ \alpha = -1,\ \lambda = 0,\ k_1 = 3,\ k_2 = -\frac{9}{4},\ k_3 = 12,\ k_4 = -12,\ \mu = 4,\ \vartheta = 1]$ for Eq. (16)

Value of $\mathfrak{Z}$	Exact value	Numerical Value	Absolute error
0	2	1.92032	0.0796816
0.1	2.39475	0.92752	1.46723
0.2	2.7599	0.256607	2.50329
0.3	3.0741	0.0981479	2.97595
0.4	3.32807	0.0251699	3.3029
0.5	3.52319	0.0226624	3.50053
0.6	3.66731	-0.00303086	3.67034
0.7	3.7707	0.152334	3.61837
0.8	3.84334	0.825615	3.01772
0.9	3.89361	2.28397	1.60964
1	3.92806	3.77156	0.156497

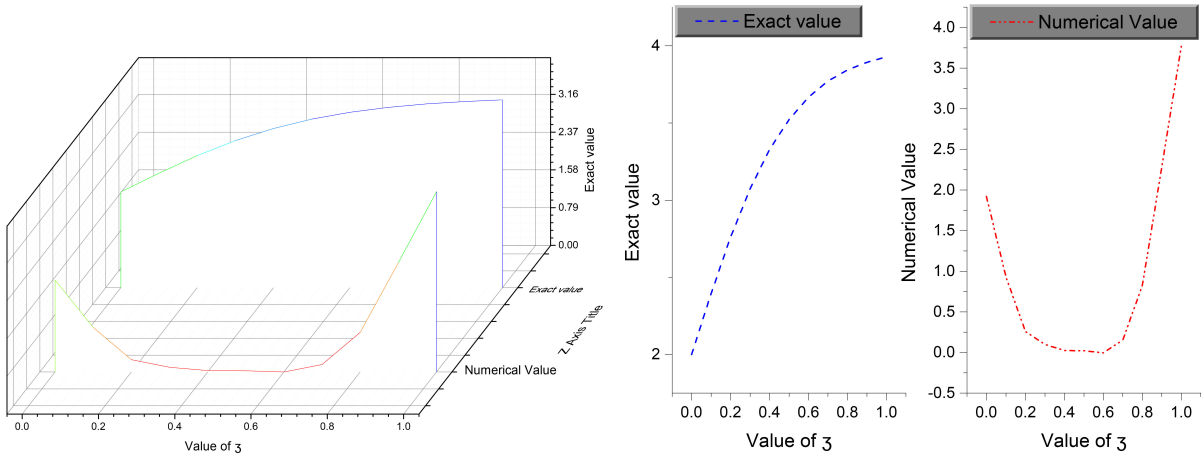

Fig. 6: Exact and numerical values by using quantic B–spline scheme for the three analytical schemes

3 Results and discussion

All computational obtained solutions are considered as optical soliton wave solutions that are used to explain the dynamical behavior of the particles in the optical waves where the optical soliton is restricted electromagnetic wave which stretches in media of nonlinear dispersive. The physical illustration of the presented figures is given as follows

1. Figs. (1, 2) show the soliton shape of the absolute, real, and imaginary solution (12) in the three–dimensional plot (a, b, c) to explain the perspective view of the solution and the absolute, real, and imaginary sketches in two–dimensional plot (d, e, f) to explain the wave propagation pattern of the wave along x axis when $[a_0 = 7,\ \alpha = -1,\ \alpha = 0.5,\ d_1 = 5,\ d_2 = 6,\ d_3 = 9,\ \mu = 4,\ l_1 = 2,\ l_2 = 3,\ \vartheta = 1]$.
2. Figs. (3, 4) show the soliton of the absolute, real, and imaginary solution (18) in the three–dimensional plot (a, b, c) to explain the perspective view of the solution and the absolute, real, and imaginary sketches in two– dimensional plot (d, e, f) to explain the wave propagation pattern of the wave along x axis when $[a_0 = 7,\ \alpha = -1,\ \alpha = 0.5,\ d_1 = 5,\ d_2 = 6,\ d_3 = 9,\ \mu = 4,\ l_1 = 2,\ l_2 = 3,\ \vartheta = 1]$.
3. Fig. 5 shows the exact and numerical solutions of Eq. (4) via cubic B - spline scheme under the following conditions $[a_0 = 2,\ \alpha = -1,\ \lambda = 0,\ k_1 = 3,\ k_2 = -\frac{9}{4},\ k_3 = 12,\ k_4 = -12,\ \mu = 4,\ \vartheta = 1]$ for Eq. (16).
4. Fig. 6 shows the exact and numerical solutions of Eq. (4) via quantic B - spline scheme under the following conditions $[a_0 = 2,\ \alpha = -1,\ \lambda = 0,\ k_1 = 3,\ k_2 = -\frac{9}{4},\ k_3 = 12,\ k_4 = -12,\ \mu = 4,\ \vartheta = 1]$ for Eq. (16).
5. Fig. 7 shows the exact and numerical solutions of Eq. (4) via septic B - spline scheme under the following conditions $[a_0 = 2,\ \alpha = -1,\ \lambda = 0,\ k_1 = 3,\ k_2 = -\frac{9}{4},\ k_3 = 12,\ k_4 = -12,\ \mu = 4,\ \vartheta = 1]$ for Eq. (16).

Table 3: Value of exact solutions, and numerical obtained solutions by septic spline scheme of (4) under the following conditions $[a_0 = 2,\ \alpha = -1,\ \lambda = 0,\ k_1 = 3,\ k_2 = -\frac{9}{4},\ k_3 = 12,\ k_4 = -12,\ \mu = 4,\ \vartheta = 1]$ for Eq. (16)

Value of $\mathfrak{Z}$	Exact value	Numerical Value	Absolute error
0	2	0.496895	1.5031
0.1	2.39475	0.347676	2.04707
0.2	2.7599	0.203475	2.55642
0.3	3.0741	0.156736	2.91736
0.4	3.32807	0.0408894	3.28718
0.5	3.52319	-0.00272479	3.52591
0.6	3.66731	0.0759522	3.59136
0.7	3.7707	0.231326	3.53938
0.8	3.84334	0.378552	3.46479
0.9	3.89361	0.650581	3.24303
1	3.92806	0.975916	2.95214

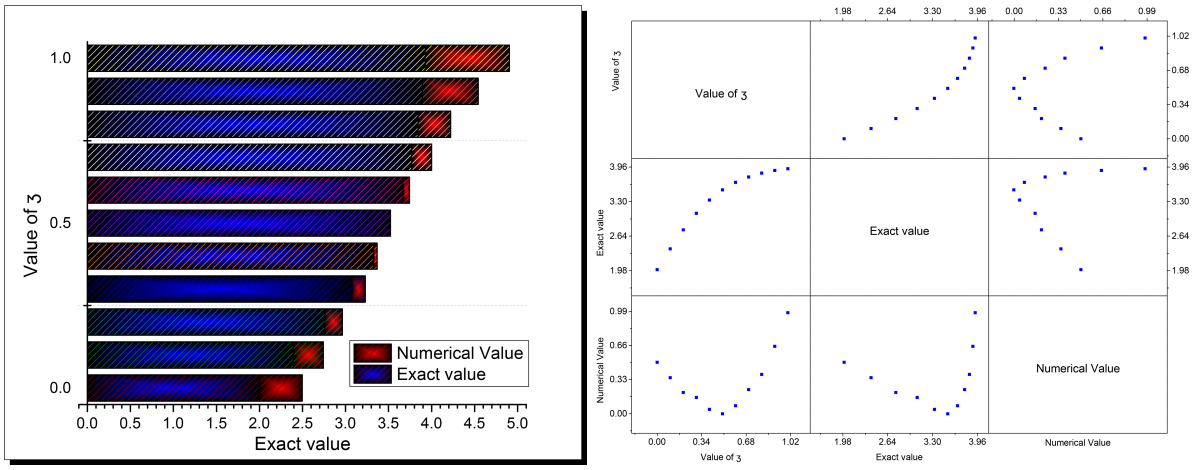

Fig. 7: Exact and numerical values by using septic B–spline scheme for the three analytical schemes

Here, the obtained computational and numerical solutions are investigated to show the novelty of our solutions as following:

1. **Computational schemes:**
   The extended simplest equation method is employed to find the exact traveling and solitary wave solutions of the higher - order dispersive cubic - quintic NLCFS equation. The employed method is considered one of the most recent derived analytical schemes. It depends on an auxiliary equation (6) that has the following general solution,

$$\mathcal{F}(\mathfrak{Z}) = \frac{\sqrt{4\alpha\mu - \lambda^2}\tan\left(\frac{1}{2}\left(\mathfrak{Z}\sqrt{4\alpha\mu - \lambda^2} + c_1\sqrt{4\alpha\mu - \lambda^2}\right)\right) - \lambda}{2\mu}, \tag{32}$$

   where c_1 is arbitrary constant. Consequently, all other obtained solutions via this method are just special case of this general solution under specific conditions.
2. **Obtained computational wave solutions:**
   - Eq. (16) is equal to Eq. (29) [42] when $[\vartheta = 0,\ -\alpha\,\mu = \chi^2 - 4\,\delta\,\varrho,\ k_1 = a_0]$.
   - All other obtained solutions are different from that obtained in [42] where the modified Khater method was employed to construct the exact traveling and solitary wave solutions.
3. **Obtained Numerical solutions:**
   Here, we explain the obtained numerical results via B - spline schemes (cubic & quantic & septic). These solutions illustrate the disadvantage of this kind of numerical schemes where the value of absolute error is relativity not small. The reason of this value is the higher and degree in Eq. (1).

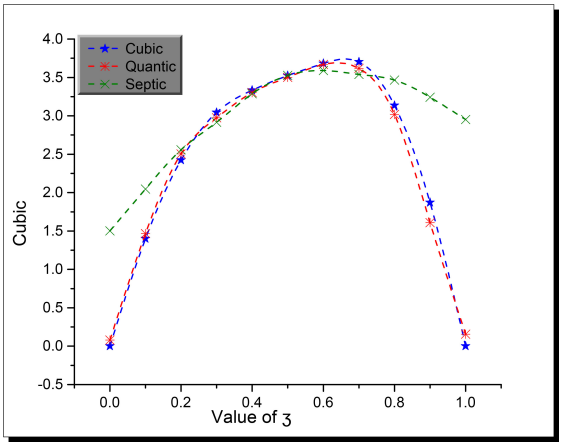

Fig. 8: The obtained absolute value of error via cubic, quantic, and septic spline schemes

4 Conclusion

This research investigated the exact traveling and solitary wave solutions of the higher-order dispersive cubic - quintic NLCFS equation via the extended simplest equation method through the conformable fractional derivative. Novel solitary wave solutions were obtained and some of them were explained by plotting them in two, three-dimensional in absolute, real, and imaginary values of these solutions. The novelty of our paper was shown by making the comparison between our obtained solutions and that were purchased in previously published articles.

References

[1] A. T. Elgendy, A.-H. Abdel-Aty, A. A. Youssef, M. A. Khder, K. Lotfy and S. Owyed, Exact solution of arrhenius equation for non-isothermal kinetics at constant heating rate and n-th order of reaction, *Journal of Mathematical Chemistry* **58** (2020) 922–938.

[2] S. Owyed, M. Abdou, A.-H. Abdel-Aty, W. Alharbi and R. Nekhili, Numerical and approximate solutions for coupled time fractional nonlinear evolutions equations via reduced differential transform method, *Chaos, Solitons & Fractals* **131** (2020) p. 109474.

[3] M. Y. Abubakar, L. T. Jung, N. Zakaria, A. Younes and A.-H. Abdel-Aty, Reversible circuit synthesis by genetic programming using dynamic gate libraries, *Quantum Information Processing* **16**(6) (2017) p. 160.

[4] E. G. Tsega, A finite Volume Solution of Unsteady Incompressible Navier-Stokes Equations using MATLAB, *Num Com Meth Sci Eng* **1** (2019) p. 117.

[5] A. Al-Saif and M. Abdul-Wahab, Application of new simulation scheme for the nonlinear biological population model, *Num. Comp. Meth. Sci. Eng* **1** (2019) 89–101.

[6] M. Abdel-Aty, M. S. Abdalla and A.-S. F. Obada, Entropy and phase properties of isotropic coupled oscillators interacting with a single atom: one-and two-photon processes, *J. Opt. B: Quantum Semiclass. Opt.* **4** (2002) S133–S141.

[7] M. S. Abdalla, M. Abdel-Aty and A.-S. F. Obada, Degree of entanglement for anisotropic coupled oscillators interacting with a single atom, *J. Opt. B: Quantum Semiclass. Opt.* **4** (2002) 396–401.

[8] D. Kumar, J. Singh, A. Prakash and R. Swroop, Numerical simulation for system of time-fractional linear and nonlinear differential equations, *Progr Fract Differ Appl* **5**(1) (2019) 65–77.

[9] M. Al-Refai and K. Pal, New aspects of Caputo–Fabrizio fractional derivative, *Prog. Fract. Differ. Appl* **5**(2) (2019) 157–166.

[10] O. Tasbozan, A. K. Yucel Çenesiz and O. S. Iyiola, New Analytical Solutions and Approximate Solution of the Space-Time Conformable Sharma-Tasso-Olver Equation, *Progress in Fractional Differentiation and Applications* **4**(4) (2018) 519–531.

[11] A. Hadhoud, Quintic non-polynomial spline method for solving the time fractional biharmonic equation, *Appl Math Inf Sci* **13** (2019) 507–513.

[12] J. Manafian and M. Lakestani, Dispersive dark optical soliton with Tzitzéica type nonlinear evolution equations arising in nonlinear optics, *Optical and Quantum Electronics* **48**(2) (2016) p. 116.

[13] T. Brabec and F. Krausz, Nonlinear optical pulse propagation in the single-cycle regime, *Physical Review Letters* **78**(17) (1997) p. 3282.

[14] J. Zhang, J.-Y. Yu and N. Pan, Variational principles for nonlinear fiber optics, *Chaos, Solitons & Fractals* **24**(1) (2005) 309–311.

[15] T. M. El-shahat, S. Abdel-khalek, M. Abdel-aty and A. S. F. Obada, Entropy squeezing of a degenerate two-photon process with a nonlinear medium, *Journal of Modern Optics* **50** (2003) 2013–2030.

[16] J. Chen, X. Xin and Y. Chen, Nonlocal symmetries of the Hirota-Satsuma coupled Korteweg-de Vries system and their applications: Exact interaction solutions and integrable hierarchy, *Journal of Mathematical Physics* **55**(5) (2014) p. 053508.

[17] G. W. Bluman and Z. Yang, A symmetry-based method for constructing nonlocally related partial differential equation systems, *Journal of Mathematical Physics* **54**(9) (2013) p. 093504.

[18] R. Anguelov and J. M.-S. Lubuma, Nonstandard finite difference method by nonlocal approximation, *Mathematics and Computers in simulation* **61**(3-6) (2003) 465–475.

[19] M. M. Meerschaert and C. Tadjeran, Finite difference approximations for two-sided space-fractional partial differential equations, *Applied numerical mathematics* **56**(1) (2006) 80–90.

[20] M. Dehghan, J. Manafian and A. Saadatmandi, Solving nonlinear fractional partial differential equations using the homotopy analysis method, *Numerical Methods for Partial Differential Equations: An International Journal* **26**(2) (2010) 448–479.

[21] Q. Yang, F. Liu and I. Turner, Numerical methods for fractional partial differential equations with Riesz space fractional derivatives, *Applied Mathematical Modelling* **34**(1) (2010) 200–218.

[22] G. Jumarie, Modified Riemann-Liouville derivative and fractional Taylor series of nondifferentiable functions further results, *Computers & Mathematics with Applications* **51**(9-10) (2006) 1367–1376.

[23] G. Jumarie, Table of some basic fractional calculus formulae derived from a modified Riemann–Liouville derivative for non-differentiable functions, *Applied Mathematics Letters* **22**(3) (2009) 378–385.

[24] D. Baleanu, A. Mousalou and S. Rezapour, A new method for investigating approximate solutions of some fractional integro-differential equations involving the Caputo-Fabrizio derivative, *Advances in Difference Equations* **2017**(1) (2017) 1–12.

[25] S. M. Aydogan, D. Baleanu, A. Mousalou and S. Rezapour, On approximate solutions for two higher-order Caputo-Fabrizio fractional integro-differential equations, *Advances in Difference Equations* **2017**(1) (2017) p. 221.

[26] M. Zidan, A.-H. Abdel-Aty, D. Nguyen, A. Mohamed, Y. Al-Sbou, H. Eleuch and M. Abdel-Aty, A quantum algorithm based on entanglement measure for classifying boolean multivariate function into novel hidden classes, *Results in Physics* **15** (2019) p. 102549.

[27] M. Eslami and H. Rezazadeh, The first integral method for Wu–Zhang system with conformable time-fractional derivative, *Calcolo* **53**(3) (2016) 475–485.

[28] H. Aminikhah, A. R. Sheikhani and H. Rezazadeh, Sub-equation method for the fractional regularized long-wave equations with conformable fractional derivatives, *Scientia Iranica. Transaction B, Mechanical Engineering* **23**(3) (2016) p. 1048.

[29] M. Eslami, F. S. Khodadad, F. Nazari and H. Rezazadeh, The first integral method applied to the Bogoyavlenskii equations by means of conformable fractional derivative, *Optical and Quantum Electronics* **49**(12) (2017) p. 391.

[30] H. Qin, M. Khater, R. A. Attia and D. Lu, Approximate simulations for the non-linear long-short wave interaction system, *Frontiers in Physics* **7** (2020) p. 230.

[31] C. Yue, M. M. Khater, R. A. Attia and D. Lu, The plethora of explicit solutions of the fractional KS equation through liquid–gas bubbles mix under the thermodynamic conditions via Atangana–Baleanu derivative operator, *Advances in Difference Equations* **2020**(1) (2020) 1–12.

[32] M. M. Khater, R. A. Attia and D. Lu, Computational and numerical simulations for the nonlinear fractional Kolmogorov–Petrovskii–Piskunov (FKPP) equation, *Physica Scripta* **95**(5) (2020) p. 055213.

[33] M. M. Khater, R. A. Attia, A.-H. Abdel-Aty, M. Abdou, H. Eleuch and D. Lu, Analytical and semi-analytical ample solutions of the higher-order nonlinear Schrödinger equation with the non-Kerr nonlinear term, *Results in Physics* **16** (2020) p. 103000.

[34] M. M. Khater, J. Alzaidi, R. A. Attia, D. Lu *et al.*, Analytical and numerical solutions for the current and voltage model on an electrical transmission line with time and distance, *Physica Scripta* **95**(5) (2020) p. 055206.

[35] R. A. Attia, D. Lu, T. Ak and M. M. Khater, Optical wave solutions of the higher-order nonlinear Schrödinger equation with the non-Kerr nonlinear term via modified khater method, *Modern Physics Letters B* **34**(05) (2020) p. 2050044.

[36] M. M. Khater, R. A. Attia and D. Baleanu, Abundant new solutions of the transmission of nerve impulses of an excitable system, *The European Physical Journal Plus* **135**(2) (2020) 1–12.

[37] H. Qin, R. A. Attia, M. Khater and D. Lu, Ample soliton waves for the crystal lattice formation of the conformable time-fractional (N+ 1) Sinh-Gordon equation by the modified Khater method and the Painleve property, *Journal of Intelligent & Fuzzy Systems* **38**(Preprint).

[38] L. Qian, R. A. Attia, Y. Qiu, D. Lu and M. M. Khater, The shock peakon wave solutions of the general Degasperis–Procesi equation, *International Journal of Modern Physics B* **33**(29) (2019) p. 1950351.

[39] V. Gerdjikov and A. Saxena, Complete integrability of nonlocal nonlinear Schrödinger equation, *Journal of Mathematical Physics* **58**(1) (2017) p. 013502.

[40] S.-F. Tian, Initial–boundary value problems for the general coupled nonlinear Schrödinger equation on the interval via the Fokas method, *Journal of Differential Equations* **262**(1) (2017) 506–558.

[41] M. J. Ablowitz, X.-D. Luo and Z. H. Musslimani, Inverse scattering transform for the nonlocal nonlinear Schrödinger equation with nonzero boundary conditions, *Journal of Mathematical Physics* **59**(1) (2018) p. 011501.

[42] C. Park, M. M. Khater, A.-H. Abdel-Aty, A. M. Zidan and A.-B. A. Mohamed, Dynamical analysis of the nonlinear complex fractional emerging telecommunication model with higher-order dispersive cubic-quintic, *Alexandria Engineering Journal (Accepted)* **Accepted** (2020).

[43] S. Owyed, M. A. Abdou, A.-H. Abdel-Aty, A. A. Ibraheem, R. Nekhili and D. Baleanu, New optical soliton solutions of space-time fractional nonlinear dynamics of microtubules via three integration schemes, *Journal of Intelligent & Fuzzy Systems* **38** (2020) 2859–2866.

[44] M. M. A. Khater, R. A. M. Attia, A.-H. Abdel-Aty, S. Abdel-Khalek, Y. Al-Hadeethi and D. Lu, On the computational and numerical solutions of the transmission of nerve impulses of an excitable system (the neuron system), *Journal of Intelligent & Fuzzy Systems* **38** (2020) 2603–2610.

[45] S. Bilige and T. Chaolu, An extended simplest equation method and its application to several forms of the fifth-order KdV equation, *Applied Mathematics and Computation* **216**(11) (2010) 3146–3153.

[46] İ. Aslan, A discrete generalization of the extended simplest equation method, *Communications in Nonlinear Science and Numerical Simulation* **15**(8) (2010) 1967–1973.

[47] H. Caglar, N. Caglar, M. Özer, A. Valarıstos and A. N. Anagnostopoulos, B-spline method for solving Bratu's problem, *International Journal of Computer Mathematics* **87**(8) (2010) 1885–1891.

[48] N. Caglar and H. Caglar, B-spline method for solving linear system of second-order boundary value problems, *Computers & Mathematics with Applications* **57**(5) (2009) 757–762.

[49] P. Bornemann and F. Cirak, A subdivision-based implementation of the hierarchical b-spline finite element method, *Computer Methods in Applied Mechanics and Engineering* **253** (2013) 584–598.